Molecular beam epitaxy of PbSrSe and PbSe/PbSrSe multiple quantum well structures for use in midinfrared light emitting devices

X. M. Fang,[a] K. Namjou, I-Na Chao, and P. J. McCann
School of Electrical and Computer Engineering and Laboratory for Electronic Properties of Materials, University of Oklahoma, Norman, Oklahoma 73019

N. Dai
Department of Physics and Astronomy and Laboratory for Electronic Properties of Materials, University of Oklahoma, Norman, Oklahoma 73019

G. Tor
Centre Universitaire des Sciences et Techniques (C.U.S.T.), Blaise Pascal University, 63006 Clermont-Ferrand Cedex, France

(Received 10 October 1999; accepted 10 February 2000)

PbSrSe layers and PbSe/PbSrSe multiple quantum well (MQW) structures have been grown on BaF_2 (111) substrates by molecular beam epitaxy. The lattice constant of the PbSrSe alloy was determined by x-ray diffraction, and both the refractive index and absorption edge of the PbSrSe alloy with Sr composition up to 0.23 were obtained from Fourier transform infrared transmission spectra at room temperature. MQW structures exhibit strong photoluminescence (PL) in the 3–5 μm wavelength range at room temperature. The PL intensity decreases monotonically with increasing temperature below 230 K. © *2000 American Vacuum Society.* [S0734-211X(00)04903-9]

I. INTRODUCTION

Molecular beam epitaxy (MBE) of the IV–VI binary compound PbSe and lead–alkaline–earth–chalcogenide PbSrSe alloy is motivated by their importance in developing midinfrared tunable diode lasers.[1,2] These materials are attractive from a growth point of view since both PbSe and SrSe share the rock-salt (face-centered-cubic) crystal structure and it is possible to grow PbSrSe with a high Sr solubility and a wide tunable energy band gap. Recently, MBE grown PbSe/PbSrSe MQW lasers operating in pulsed mode up to 282 K at a wavelength of $\lambda=4.2$ μm have been demonstrated.[2]

It is known that the presence of Auger recombination in narrow gap semiconductors is the major intrinsic limitation in achieving midinfrared tunable diode lasers with high operating temperatures. Recently, much progress has been made in achieving high power emission and high operating temperature with III–V semiconductor quantum cascade laser structures and type-II antimonide quantum well systems.[3–5] IV–VI semiconductors have several unique properties that make them attractive for midinfrared laser fabrication. In contrast to III–V and II–VI semiconductors, IV–VI lead salts have a band structure with mirror-image *L*-point bands that is highly favorable for Auger suppression. In this work, PbSe/PbSrSe MQW structures have been grown on BaF_2 (111) substrates. Strong photoluminescence (stimulated emission) has been observed from these structures in the wavelength range of 3–5 μm at room temperature, which supports the speculation made recently that Auger recombination in IV–VI semiconductors in the wavelength range of 3–5 μm will not prevent quantum structures of these materials from achieving room temperature laser operation.[6] Refractive indices and absorption edge energies for PbSrSe have also been obtained from Fourier transform infrared (FTIR) transmission experiments.

II. MBE GROWTH PROCEDURE

All structures were grown on BaF_2 (111) substrates in a GEN II MBE system. BaF_2 substrates were freshly cleaved from a (111)-oriented 1 cm×1 cm ingot and mounted onto a uniblock with a silicon backing plate. Before being transferred to the growth chamber, the substrate was outgased in the preparation chamber at 200 °C for 1 h.

After the BaF_2 substrate was transferred into the growth chamber, the substrate temperature was ramped up to 550 °C until a sharp BaF_2 (1×1) reflection high-energy electron diffraction (RHEED) pattern appeared. A 100-nm-thick BaF_2 buffer layer was first grown on the substrate at 500 °C. The growth temperature was measured using a thermocouple. X-ray diffraction measurements showed that the growth of a BaF_2 buffer layer could reduce the linewidth of (222) diffraction of the subsequently grown PbSrSe layer by 30%–50%. A 3-μm-thick PbSrSe layer was then grown on top of the BaF_2 buffer layer at 360 °C. The growth of PbSrSe was carried out by evaporating PbSe and elemental Sr sources. The Sr composition was controlled by varying the Sr to PbSe flux ratio. The actual Sr content was determined from x-ray diffraction measurements. An additional Se source was used to control the stoichiometry of PbSe and PbSrSe layers and keep the surface under Se rich conditions. A valved cracker cell was used to produce a Se flux of 10% relative to the total PbSe and Sr fluxes. The typical beam equivalent pressure of PbSe is about 1.56×10^{-6} Torr. The PbSe and PbSrSe growth rates were both about 180 Å/min.

[a]Corresponding author; present address: Quantum Epitaxial Designs, Inc., 119 Technology Drive, Bethlehem, PA 18015; electronic mail: fang@qedmbe.com

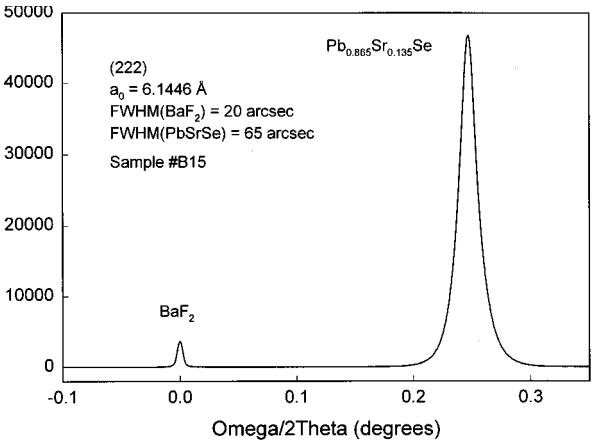

FIG. 1. X-ray diffraction rocking curve for a 3.4-μm-thick PbSrSe epilayer grown on BaF_2 (111).

To grow a MQW structure, 10–40 periods of PbSe/PbSrSe were grown on top of the PbSrSe buffer layer at 360 °C. The thicknesses of the PbSe quantum well and PbSrSe barrier were in the range of 40–200 and 400–500 Å, respectively. To prevent the final PbSrSe layer from being oxidized, a 10-nm-thick PbSe cap layer was grown on top of either a single PbSrSe layer or a PbSe/PbSrSe MQW structure. All the PbSe and PbSrSe layers are undoped.

Growth was monitored *in situ* using the RHEED technique. *Ex situ* structural characterization of the epilayers was performed using a Philips high-resolution x-ray diffraction system with a four-crystal Ge (220) monochromator. Fourier transform infrared (FTIR) transmission measurements were carried out using a Bio Rad spectrometer (FTS-60A) with a wave number range of 50–6000 cm^{-1}. Photoluminescence (PL) measurements were performed using a modular FTIR spectrometer (Oriel, MIR8000). MBE samples were illuminated with a 972 nm InGaAs laser. The injection current for the InGaAs pump laser was 500 mA producing about 250 mW of power. The unfocused laser, located about 10 mm from the sample at about a 45° angle, produced a spot size of about 2 mm×7 mm on the sample surface. An average power density of about 1.8 W/cm^2 is thus estimated. The PL setup and data acquisition are described in detail elsewhere.[7]

III. RESULTS AND DISCUSSION

A. PbSrSe grown on BaF_2 (111)

The initial growth of PbSrSe on BaF_2 proceeded via a three-dimensional growth mode. However, the electron diffraction spots were replaced by streaks after a few hundred angstroms of PbSrSe were deposited.

Figure 1 shows the x-ray diffraction rocking curve for a $Pb_{0.865}Sr_{0.135}Se$ epilayer grown on BaF_2 (111). The typical line width of the PbSrSe (222) diffraction peak is in the range of 50–70 arcsec for layers with thicknesses of 2–3 μm and with Sr composition less than 0.23. Since the lattice constant of BaF_2 substrate material is known, the BaF_2 diffraction peak shown in Fig. 1 can be used as a reference to determine the absolute diffraction angle of the $Pb_{0.865}Sr_{0.135}Se$ peak. The lattice constant of the $Pb_{0.865}Sr_{0.135}Se$ epilayer can thus be calculated using Bragg diffraction law. The lattice constant of PbSrSe has been determined for various epilayers in this way. The results are listed in Table I. For epilayers with small Sr composition, it is a good assumption that Vegard's law applies to the lattice constant of PbSrSe alloy. Since the lattice constants of PbSe and SrSe have been obtained from x-ray diffraction, the Sr composition of PbSrSe alloy can be determined by applying Vegard's law. The variation of the lattice constant with Sr composition can be formulated as follows:

$$a = 6.126 + 0.123x(\text{Å}) \quad \text{for } 0 \leqslant x \leqslant 0.23. \tag{1}$$

The lattice constant of PbSe determined in this work is in good agreement with the value 6.126 Å used in prior work.[8] The corresponding Sr to PbSe flux ratios used to adjust the Sr composition during the growth are also listed in Table I for reference.

TABLE I. Variations of the lattice constant and absorption edge of PbSrSe epilayers as a function of Sr composition. The corresponding Sr to PbSe flux ratios used to adjust the Sr composition in the growth are also included.

Sr composition	Sr to PbSe flux ratio (%)	Lattice constant (Å)	Absorption edge (eV)
0.0	0.0	6.1260	0.277
0.068	3.0		0.451
0.135	6.0	6.1446	0.577
0.230	10.0	6.1563	0.716
1.0		6.2509	

Figure 2 shows the FTIR transmission spectra for two PbSrSe samples with Sr compositions of 0.068 and 0.230, respectively. The spectra were obtained at room temperature. It can be seen that the spectra are dominated by the well-pronounced Fabry–Perot (FB) interference below the ab-

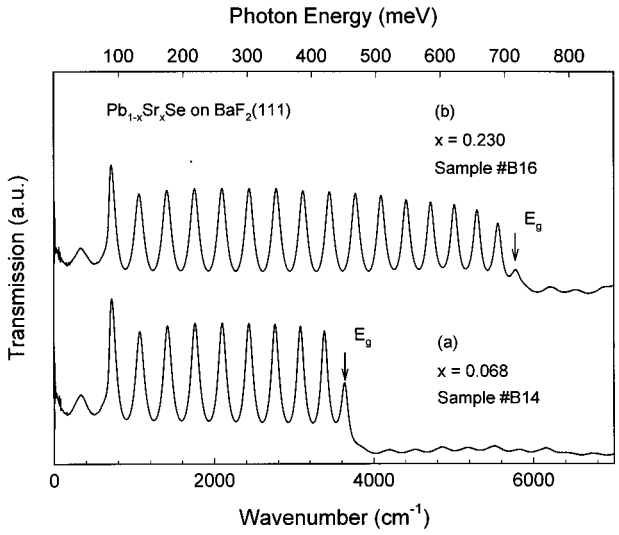

FIG. 2. FTIR transmission spectra of two $Pb_{1-x}Sr_xSe$ epilayers obtained at room temperature. (a) $x=0.068$, layer thickness of 3.3 μm; (b) $x=0.230$, layer thickness of 3.8 μm.

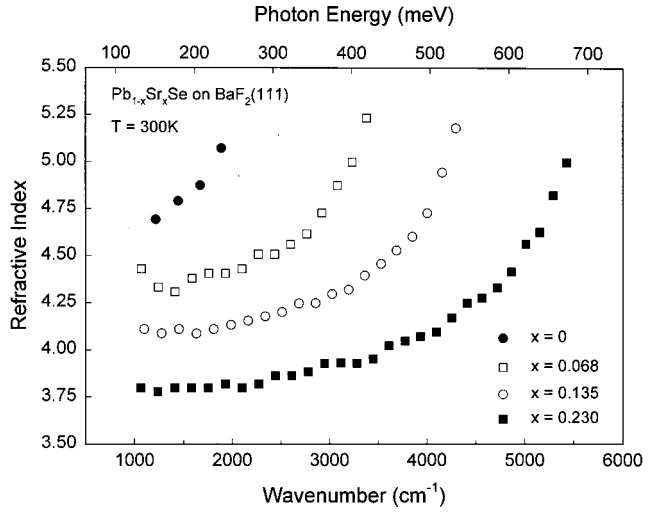

FIG. 3. Variation of refractive index in PbSrSe as a function of Sr composition.

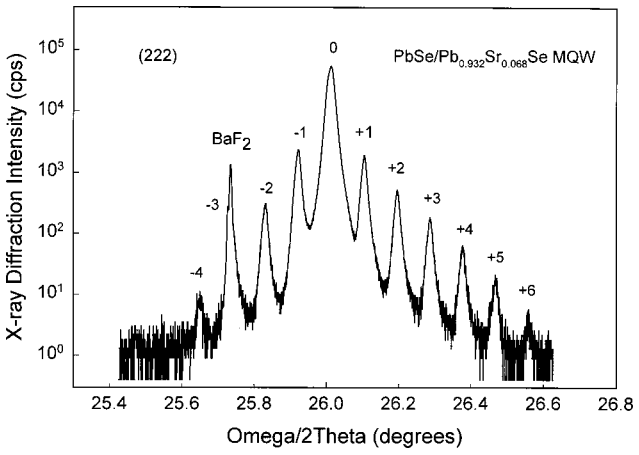

FIG. 4. X-ray diffraction rocking curve for a 40-period PbSe(10 nm)/$Pb_{0.932}Sr_{0.068}Se$ (50 nm) MQW structure grown on BaF_2 (111).

sorption edges. The FB fringes are still present above the absorption edges though they are much weaker. The shift in the absorption edge with increasing Sr composition is also clearly seen in the spectra. The absorption edge was determined from the first transmission maximum as indicated in Fig. 2. Absorption edge values for each layer are listed in Table I. The uncertainty in determining the absorption edge was estimated to be less than 10 meV. The variation of the absorption edge with Sr composition was fitted using the following quadratic function:

$$E_g = 0.278 + 2.725x - 3.579x^2 (\text{eV}) \quad \text{for } 0 \leqslant x \leqslant 0.23. \qquad (2)$$

Like other ternary lead chalcogenide alloys,[9,10] PbSrSe epilayers also show nonlinear dependence of the absorption edge on Sr composition.

It is known that the presence of the FB interference below and above the absorption edge allows determining the refractive index of an epilayer. One of the commonly used methods is to determine the refractive index by using the formula $\Delta\nu = 1/(2nd)$, where $\Delta\nu$ is the period of interference fringes, n is the refractive index, and d is the thickness of the epilayer.[11] Another method is to fit a transmission spectrum using a derived theoretical model based on the energy band structure of the material investigated.[12] The advantage of the second method is that it allows both the refractive index and the absorption coefficient to be determined. In this work, the first method was used to determine the refractive index of PbSrSe epilayers due to its simplicity. The results are shown in Fig. 3. The refractive index of PbSe epilayer determined in this work is in good agreement with Zemel *et al.*'s result[13] in the photon energy range below the absorption edge.

B. PbSe/PbSrSe MQW structures grown on BaF_2 (111)

Figure 4 shows an x-ray diffraction rocking curve for a PbSe/PbSrSe MQW structure grown on BaF_2 at 360 °C. Satellite reflection peaks with the order up to 7 were clearly seen from the MQW sample indicating the high quality of the sample.

Figure 5 shows a PL spectrum taken at 25 °C for a 40-period PbSe (20 nm)/$Pb_{0.932}Sr_{0.068}Se$(50 nm) MQW structure grown on BaF_2 (111). The spectrum exhibits several distinct emission peaks in the 3–5 μm wavelength range. These are Fabry–Perot interference fringes due to resonance in the optical cavity formed by the layer. The left side of the strongest peak near 2400 cm^{-1} is somewhat distorted due to absorption by atmospheric CO_2 in the open path PL setup. The presence of the FB interference fringes indicates that the emission process is dominated by stimulated emission because spontaneous emission cannot cause interference.[14] The inset shown in Fig. 5 is the variation of PL intensity as a function of the sample temperature. It can be seen that the PL intensity reaches maximum in the temperature range of

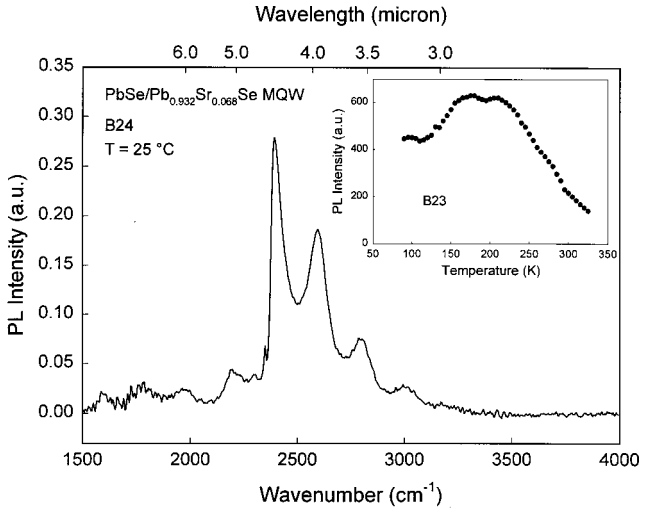

FIG. 5. PL spectrum taken at 25 °C for a 40-period PbSe (20 nm)/$Pb_{0.932}Sr_{0.068}Se$ MQW structure. Inset: The temperature dependence of PL intensity for a 40-period PbSe (10 nm)/$Pb_{0.932}Sr_{0.068}Se$ MQW structure.

170–210 K. Note that at temperatures below 170 K, the PL intensity drops as the temperature decreases. Above 230 K the PL intensity decreases monotonically as the temperature increases. Above room temperature the sample still shows considerable PL intensity, about 20% of the maximum value obtained at low temperature. The observation of PL emission at room temperature indicates that Auger recombination does not limit the emission process in the wavelength range from 3 to 5 μm for PbSe/PbSrSe MQW structures. Recently Findlay *et al.* measured the Auger recombination rates in PbSe and found that the Auger coefficient (with a value of about $8\times10^{-28}\,\mathrm{cm}^6\,\mathrm{s}^{-1}$) for PbSe is between one and two orders of magnitude lower than for II–VI and III–V semiconductors of comparable band gap.[15] The room temperature PL results suggest that Auger recombination in IV–VI semiconductors in the wavelength range of 3–5 μm will not prevent PbSe/PbSrSe quantum well structures from achieving room temperature laser operation.

IV. CONCLUSION

Single PbSrSe epilayers and PbSe/PbSrSe MQW structures have been grown on BaF_2 substrates, Structural and optical properties of the epilayers have been characterized. The refractive indices of PbSrSe alloys for composition less than 0.23 has been obtained at room temperature. The PbSe/PbSrSe MQW structure exhibits strong photoluminescence in 3–5 μm at room temperature.

ACKNOWLEDGMENTS

This work is supported by the Oklahoma Center for the Advancement of Science and Technology (OCAST), Contract No. AR6-054 and the National Science Foundation, grant No. DMR-98023961.

[1]B. Spanger, U. Schiessl, A. Lambrecht, H. Böttner, and M. Tacke, Appl. Phys. Lett. **53**, 2582 (1988).
[2]Z. Shi, M. Tacke, A. Lambrecht, and H. Böttner, Appl. Phys. Lett. **66**, 2537 (1995).
[3]D. Hofstetter, J. Faist, M. Beck, A. Müller, and U. Oesterle, Appl. Phys. Lett. **75**, 665 (1999).
[4]A. Tredicucci, C. Gmachl, F. Capasso, D. L. Sivco, A. L. Hutchinson, and A. Y. Cho, Appl. Phys. Lett. **74**, 638 (1999).
[5]W. W. Bewley, C. L. Felix, E. H. Aifer, I. Vurgaftman, L. J. Olafsen, J. R. Meyer, H. Lee, R. U. Martinelli, J. C. Connolly, A. R. Sugg, G. H. Olsen, M. J. Yang, B. R. Bennett, and B. V. Shanabrook, Appl. Phys. Lett. **73**, 3833 (1998).
[6]R. Klann, T. Hofer, R. Buhleir, T. Elsaesser, and J. W. Tomm, J. Appl. Phys. **77**, 277 (1995).
[7]P. J. McCann, K. Namjou, and X. M. Fang, Appl. Phys. Lett. **75**, 3608 (1999).
[8]P. J. McCann, J. Fuchs, Z. Feit, and C. G. Fonstad, J. Appl. Phys. **62**, 2994 (1987).
[9]Dale L. Partin, Semicond. Semimet. **33**, 311 (1991).
[10]X. M. Fang, I-Na Chao, B. N. Strecker, P. J. McCann, S. Yuan, W. K. Liu, and M. B. Santos, J. Vac. Sci. Technol. B **16**, 1459 (1998).
[11]H. R. Riedl and R. B. Schoolar, Phys. Rev. **131**, 2082 (1963).
[12]P. J. McCann, L. Li, S. Yuan, and J. E. Furneaux, *Narrow Gap Semiconductors 1995* (Institute of Physics, London, 1995), p. 150.
[13]J. N. Zemel, J. D. Jensen, and J. D. Schoolar, Phys. Rev. A **140**, 330 (1965).
[14]J. W. Tomm, K. H. Hermann, and A. E. Yunovich, Phys. Status Solidi A **122**, 11 (1990).
[15]P. C. Findlay, C. R. Pidgeon, R. Kotitschke, A. Hollingworth, B. N. Murdin, C. J. G. M. Langerak, A. F. G. van der Meer, C. M. Ciesla, J. Oswald, G. Homer, G. Springholz, and G. Bauer, Phys. Rev. B **58**, 12908 (1998).